RSC Advances

This is an *Accepted Manuscript*, which has been through the Royal Society of Chemistry peer review process and has been accepted for publication.

Accepted Manuscripts are published online shortly after acceptance, before technical editing, formatting and proof reading. Using this free service, authors can make their results available to the community, in citable form, before we publish the edited article. This *Accepted Manuscript* will be replaced by the edited, formatted and paginated article as soon as this is available.

You can find more information about *Accepted Manuscripts* in the **Information for Authors**.

Journal Name

ARTICLE

Alkylated Cage Silsesquioxanes: A Comprehensive Study of Thermal Property and Self-Assembled Structure

Lei Wang,[a] Yoshihito Ishida,[b] Rina Maeda,[a,c] Masatoshi Tokita,[a] and Teruaki Hayakawa[a,d]*

Derivations of mono-substituted polyhedral oligomeric silsesquioxanes (POSS) with long aliphatic chains were synthesized and self-assembled structures were investigated. The effects of the alkyl chains length and branching on the thermally self-assembling behaviors of the POSS derivatives were examined by differential scanning calorimetry (DSC) and polarized optical microscopy (POM). In addition, small- and wide-angle X-ray scattering (SAXS/WAXS) as well as transmission electron microscopy (TEM) were employed to elucidate their self-assembled morphologies. Long-range straight ordered lamellar structure with sharp boundaries could be reliably formed in the bulk samples of alkylated cage silsesquioxanes by thermal annealing. Furthermore, this research demonstrates an approach to precisely control the feature size at nanometer scale by carefully tuning parameters of alkyl chain length and branching number.

Introduction

Nanofabrication by block copolymer (BCP) self-assembly has been one the greatest achievements in nanotechnologies.[1-5] Various self-assembled structure have been reported by controlling the composition of BCPs.[4,5] However, the self-assembling structural control remains a grand challenge in sub-10 nm scale,[6] especially to the fabrication of long-range ordered nanopattern.[7]

Giant molecules[8-14] with precisely defined chemical structures have been explored as new approaches to the fabrication of engineered hierarchical structures with sub-10 nm feature sizes and sharp boundaries by the self-assembly, which are difficult to achieve with traditional diblock copolymers.[8] Molecular nanoparticles (MNPs) or "nanoatoms"[9] are shape- and volume-persistent nano-objects with well-defined molecular structures and specific symmetries, which have been utilized as elemental molecular nano-building blocks for the precision synthesis of giant molecules. Among the MNPs, polyhedral oligomeric silsesquioxane (POSS) has attracted intensive interest over the last several decades due to its unique structure and properties.[16, 17] POSS exhibits a well-defined molecular structure with the formula $(RSiO_{3/2})_n$, in which organic substitutes R are attached to a silicon-oxygen cage.[16] This intramolecular organic-inorganic hybrid structure endows POSS with extraordinary properties such as excellent thermal stability,[18] an ultra low dielectric constant,[19] and outstanding oxygen plasma etching resistance.[20] In addition, the surface groups can easily be chemically modified, which makes POSS a nearly perfect nanobuilding block for the fabrication of precisely defined giant molecules.[8-15]

A series of POSS-containing giant surfactants were synthesized and their self-assembled structures were reported by Cheng and coworkers.[8] Polystyrene with narrow molecular weight dispersity was synthesized and tethered to hydrophilic POSS via click chemistry. The volume fraction could be tuned by the repeat unit of styrene or the numbers of cage silsesquioxane. These giant surfactants could produce various self-assembled nanostructures, which resemble the self-assembled structures of BCPs except smaller feature size. As it claimed, giant surfactants bridge the gap in the sizes of the self-assembled structures between small-molecule surfactants and block copolymers and demonstrate a duality of both materials in terms of their self-assembly behaviors.[8,9]

Although polystyrene,[8-10,12,14] poly(ethylene glycol),[15] polypetides,[24-26] liquid crystalline mesogens,[27-29] and other building blocks have been reported to form POSS-containing self-aggregated structures, functionalizing the building block with alkyl chains is the most common strategy in their molecular design.[30-43] Notably, long *n*-alkanes exhibit

monodispersed molecular weights and exact chemical structures and therefore may provide an approach to control the self-assembled structure at nanometer scale by molecular design.

There are now numerous methods available to incorporate alkyl chains into POSS, such as hydrolysis,[34] hydrosilylation, [32, 37] and Friedel-Crafts alkylation reactions.[36] Recently, in order to understand the crystalline packing and thermal behavior of a homologous series of *n*-alkyl-substituted POSS derivatives were reported.[31] However, the previous research mostly focused on simultaneous multisite functionalized POSS. To the best of our knowledge, there have been few reports addressing the self-assembly structure and morphology of mono-substituted alkylated cage silsesquioxane. Moreover, from the standpoint of synthesis of POSS derivatives, mono-substituted POSS was expected to give an easier purification process than multi-substituted one, as shown in a dendrimer synthesis.

We previously investigated the incorporation of a wedge-shaped building block, 3,4,5-tris(octadecyloxy)benzyl, into POSS.[35] This giant molecule with exact molecular weight and chemical structure, **1**, as shown in Scheme 1. Compare with these reported giant molecules, alkylated POSS was synthesized by precision organic synthesis instead of living polymerization on the basis of that primary chemical structure is thought to vital to the giant molecular self-assembled structure[9] especially when the feature size shrinks to sub-10 nm scale. Our study showed that the alkylated POSS could form a well-defined self-assembled structure with a periodicity of 5.3 nm in the bulk sample.[35]

As far as we know, the number, size (length), and even shape of the flexible chains will affect the thermal properties, morphology, and assembly.[39] Therefore, the proper selection of flexible chains in suitable numbers would be valuable in fabricating ordered self-assembled structures with tunable periodicities and thermal behaviors. However, despite this study and many others reported in the literature, a comprehensive understanding of the structure and molecular packing of mono-substituted alkylated POSS crystals and the principles that can guide molecular design are still lacking.

Thus, we report herein a novel library of branched alkylated cage silsesquioxanes with different alkyl chain lengths and branch numbers (**1–5** in Scheme 1), we investigated their thermal properties, self-assembled structures as well as structure-property relationship with the expectation that this research could provide a guide to the future molecular design of this series of alkylated POSS derivatives.

Results and discussion

In this report, we successfully attached branched alkyl chains to the aminopropylisobutyl POSS core via amidation reaction. The giant molecules were denoted as POSS-C_X-YA, where X refers to the alkyl chain length and Y refers to the number of branching substituents. By varying the alkyl chain length (C_6, C_{12}, and C_{18}) and the number of branches (1, 2, and 3), a library of alkylated POSS analogues was obtained: POSS-

C_{18}-3A (**1**), POSS-C_{12}-3A (**2**), POSS-C_6-3A (**3**), POSS-C_{18}-2A (**4**), and POSS-C_{18}-1A (**5**). The alkyl chain with different length (C_6, C_{12} and C_{18}) was expected to provide an insight to study the influence of alkyl chain length on the periodicity of self-assembled structure. Therefore, it demonstrates an approach to tailor feature size by choosing appropriate aliphatic tail. Meanwhile, the number of branches is taken into consideration since it may exert an influence on the intermolecular forces and therefore, by some extent, dictate the regularity of self-assembled structure.

These alkylated POSS derivatives were synthesized according to the method described in the supporting information (refer to Scheme S1). The resulting products were characterized by ^{1}H, ^{13}C NMR and matrix assisted laser desorption ionization time-of-flight mass spectrometry (MALDI-TOF-MS). Detailed synthesis and characterization results are shown in the supporting information.
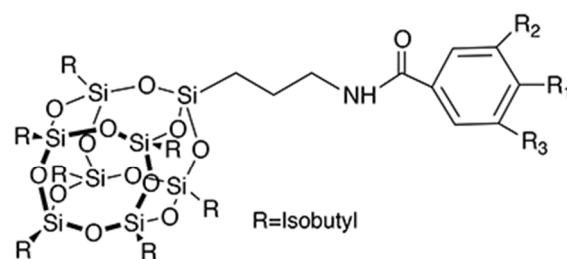
1	$R_1=R_2=R_3=OC_{18}H_{37}$	POSS-C_{18}-3A
2	$R_1=R_2=R_3=OC_{12}H_{25}$	POSS-C_{12}-3A
3	$R_1=R_2=R_3=OC_6H_{13}$	POSS-C_6-3A
4	$R_1=R_2=OC_{18}H_{37}$ $R_3=H$	POSS-C_{18}-2A
5	$R_1=OC_{18}H_{37}$ $R_2=R_3=H$	POSS-C_{18}-1A

Scheme 1. Chemical structures of alkylated POSS derivatives (**1–5**)

Thermal properties

It is very important to investigate thermal behavior in detail for self-assembly study of newly synthetic giant molecules. The temperature of the formation of mesophases (T_1, T_2 and T_3) and the isotropization of the mesophases (T_m), as well as the corresponding enthalpy changes were measured via DSC at a heating rate of 10 ºC/min and are listed in Table S1 (refer to the supporting information). Prior to each measurement, each sample was cooled from isotopic state to ambient at the rate of 10 ºC/min in order to erase any thermal history.

As shown in Figure 1, these large endotherms represent the melting of the crystalline structure, that is, a solid-liquid phase transition. However, minor enthalpy transitions (labeled as T_1 and T_2 in Figure 1), are observed from all curves. Two quite pronounced peaks representing minor thermal transitions occur at 68 ºC (1.39 KJ/mol) and 80 ºC (0.377 KJ/mol) in the thermogram of **1**. As the alkyl chain lengths decrease to C_{12} and C_6, these transition peaks can still be observed at 16 ºC (2.28 KJ/mol) and 25 ºC (9.80 KJ/mol) for POSS-C_{12}-3A, and 1 ºC

(0.869 KJ/mol) and 13 ºC (0.805 KJ/mol) for POSS-C$_6$-3A. These minor transitions in the alkylated POSS derivatives during the heating process can be interpreted by the rotation or minor structural reordering of the long alkyl chain arms that are not tethered to the POSS.[34] This phenomenon is often described as a solid-solid phase transition, which can also be observed in the thermal behavior of linear long alkyl chain substituted POSS reported by Heeley and coworkers.[34] Some minor structural disorder exists in the chain when packing together due to the rotation or chain translation. Chain mobility concomitantly with alkyl chain length; hence, more rotations of the long alkyl chain ends are permitted. This provides a reasonable explanation to the fact that the enthalpy transitions observed from the DSC curves are amplified with increasing alkyl chain length.[34]
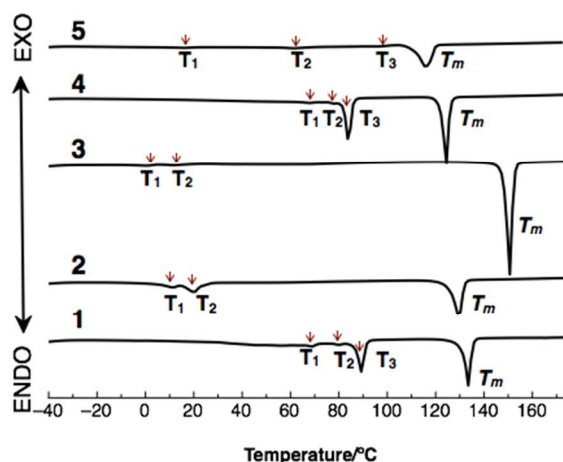

Figure 1. DSC heating thermograms of the second cycle showing enthalpy transitions for **1** (POSS-C$_{18}$-3A); **2** (POSS-C1$_2$-3A); **3** (POSS-C$_6$-3A); **4** (POSS-C$_{18}$-2A); and **5** (POSS-C$_{18}$-1A). The melting temperature, the transitions for rotator phase and solid-solid transition temperature are denoted as T_m, T_1, T_2 and T_3, respectively.

DSC was also employed to study the thermal behavior of the C$_{18}$-alkylated POSS derivatives with different numbers of branches (**1**, **4**, and **5**). Figure 1 shows the heating thermograms for POSS-C$_{18}$-3A (**1**), POSS-C$_{18}$-2A (**4**), and POSS-C$_{18}$-1A (**5**), where **1, 4** exhibit similar thermal behaviors and another major endotherm (labeled T$_3$ in each curve). Although the enthalpy is relatively small (0.735 KJ/mol), a minor thermal transition could be also detected at 99 ºC during the heating process in the sample of POSS-C18-1A (**5**). Thus, this additional thermal transition and new mesophase are supposed to be formed due to the incorporation of the C$_{18}$ alkyl chain. In previous research,[35] we reported the structural evolution of **1** during the heating process. The POM technique was used to observe the optical texture of **1**, revealing spherocrystals at room temperature. During heating upon the POM-equipped hot stage, we observed the disappearance of these spherulites, indicating the formation of a new phase at 89 °C (25.9 KJ/mol). A similar process was

observed for POSS-C$_{18}$-2A, where a highly ordered spherulite underwent an obvious solid-solid transition at 87 ºC (19.9 KJ/mol) (see Figure S5 in the supporting information). At room temperature, this POSS exists in a rigid crystalline state in which all the alkyl chains have *trans* conformations.[20] The alkyl substituents adopt disordered structures at elevated temperature, which results in the disappearance of the spherocrystals. As the temperature increases further, the molecular arrangement changes to a less ordered packing structure. When the temperature is increased to 133 ºC, **1** was converted to a fluid state.

The melting temperatures determined by DSC together with the POM observations are summarized in the fifth column of Table S1 (refer to supporting information). As shown in Figure 1, a clear trend may be observed in which T_m increases with decreasing alkyl chain length. This may be the weaker intermolecular force of alkyl chain becomes dominant in the whole alkylated POSS as the alkyl chain length increases. For compounds **1**, **4**, and **5**, the melting points decrease with fewer branches due to the lower molecular weight and weaker CH$_2$-CH$_2$ interactions. This can lead to weakening the intermolecular forces between POSS cages. This initial result indicates the alkyl chain lengths and chain numbers dictate the molecular packing and, hence, the crystalline structures in the POSS cage systems. We will next discuss the packing morphology and our proposed molecular packing model.
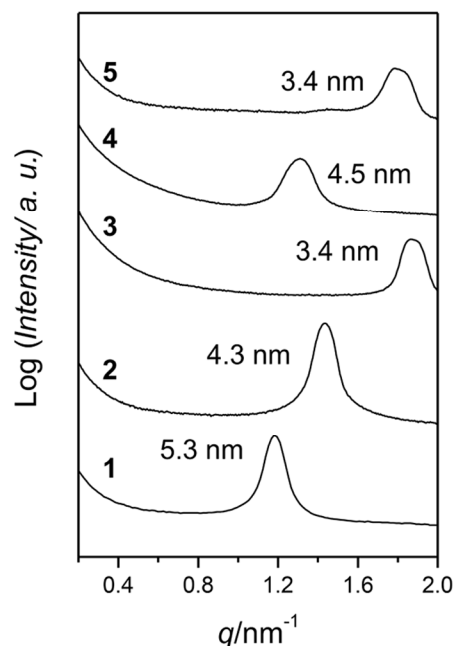
Molecular packing characterization

Figure 2. SAXS profiles showing the first order *d*-spacing lengths of **1** (POSS-C$_{18}$-3A); **2** (POSS-C$_{12}$-3A); **3** (POSS-C$_6$-3A); **4** (POSS-C$_{18}$-2A); and **5** (POSS-C$_{18}$-1A).

To investigate the influence of the alkyl chain length on periodicity of the self-assembled structure, the SAXS profiles

of **1**–**3** were obtained (Figure 2). Samples were annealed by slowly decreasing the temperature at a rate of 0.1 ºC/min from the isotropic state to 30ºC. POSS-C_{18}-3A (**1**) exhibits a larger first order d-spacing than **2** and **3**; its longer alkyl chains would eventually result in a longer first order d-spacing. For the C_{18}-substituted POSS analogues **1**, **4**, and **5**, the compounds with fewer branches exhibit smaller d-spacings for the major peak. A promising explanation lies in the reduction of steric effects, which may lead to closer packing of the less-substituted C_{18}-alkylated POSS compounds, and hence, shorten the d-spacing of the major peak.

The plot of the d-spacing of first order with respect to even carbon number of each branch in three-armed alkylated POSS derivatives (**1**, **2**, and **3**) is shown in Figure 3. The first order d-spacing plot shows a linear relationship with respect to the increasing carbon number of each chain. Moreover, the gradient of the linear fit to the plot is 0.158 nm per CH_2 group. Similar trends could be found in the cases of long alkane chains and homologous series of n-alkyl-substituted POSS derivatives (T_8C_{18}, T_8C_{16} and T_8C_{14})[34] where the length increases by 0.127 nm or 0.250 nm per carbon number, respectively. Such gradient, 0.158 nm per carbon number, suggests the long alkyl chains of neighboring layers probably partially penetrate each other in the formation of the self-assembled structure. Interestingly, to POSS-C_{12}-3A (**2**) and POSS-C_{18}-2A (**4**), which exhibit the same carbon number, the values of the first order d-spacing are almost the same. Similar phenomenon could also be observed from POSS-C_6-3A (**3**) and POSS-C_{18}-1A (**5**). Notably, the relationship of the first order d-spacing with the carbon number could provide a method to tailor the self-assembled feature sizes of alkylated POSS by thoroughly choose the alkyl chain length.
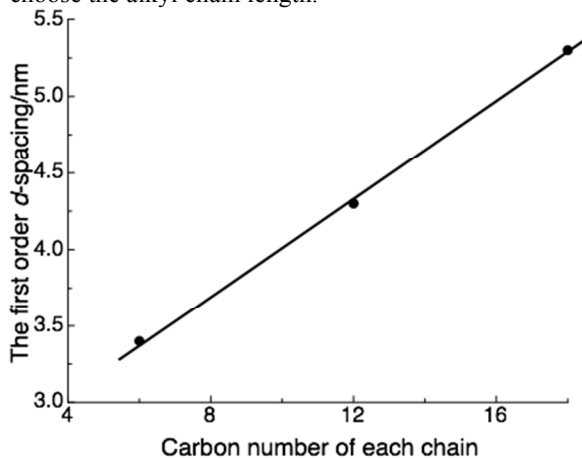

Figure 3. Plot of first order of d-spacing with length of three-arm-substituted alkylated POSS derivatives.

In order to obtain a more detailed analysis of the molecular packing of these alkylated POSS derivatives, TEM was employed to investigate the morphologies of solvent evaporation induced self-assembly (EISA) samples and thermally annealed samples that were obtained by evaporation

from chloroform or by decreasing the temperature from the isotropic state to 30ºC at a rate of 0.1 ºC/min, respectively.
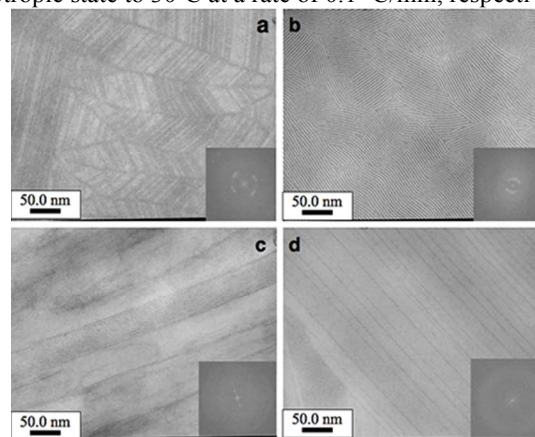

Figure 4. TEM images of solvent evaporation induced self-assembly (EISA) samples obtained by slow evaporation from chloroform: (a) POSS-C_6-3A; (b) POSS-C_{12}-3A; (c) POSS-C_{18}-2A; and (d) POSS-C_{18}-1A. FFT patterns are also shown as the inset in each figure.

In the TEM images of the samples obtained by evaporation induced self-assembly, poorly ordered lamellar patterns at nanometer scale could be clearly observed. The morphologies of POSS-C_6-3A (**3**) and POSS-C_{12}-3A (**2**) (shown as (a) and (b) in Figure 4) are lamellar structures with clear grain boundaries but just limited to small domains. Fast Fourier-transform (FFT) patterns of **3** and **2** were shown in the insertion of TEM images. From the center outward, we see arcs and wide halo. This wide halo is thought to be caused by instrument undulation at high magnification. The occurrence of the wide arcs indicates that the molecular arrangement is not well-organized.[45] Similarly, the TEM images of **4** and **5** show lamellar structure but which lack of long-range order at large area. The disappearance of sharp dots and arcs also confirms the alkylated POSS is not organized at highly orderly fashion.

Thermally annealed samples were obtained by slowly decreasing the temperature from the isotopic state to 30 ºC at the rate of 0.1 ºC/min during the cooling cycle. Figure 5 reveals well-defined lamellar patterns over large areas, shown as an alternating arrangement of bright and dark streaks. The dark and bright streaks correspond to the POSS and long alkyl chain domains, respectively. In addition, the occurrence of the highly ordered spots in the FFT diagrams reveals that the lamellar arrangements retain a high degree of periodicity. Long-range ordered lamellar structure could be easily observed from Figure 5 (a)-(d). Surprisingly, even in the case of non-branched, mono-substituted POSS, POSS-C18-1A, the nanopattern shown Figure 5d and Figure 6d is also well-defined. In general, these alkylated POSS derivatives, especially even non-branched, mono-substituted POSS-C18-1A (**5**), exhibit long-range ordered lamellar structure with sharp boundaries under thermal annealing conditions due to the strong microphase separation driving force determined by sufficient intermolecular forces between POSS and alkyl chain.
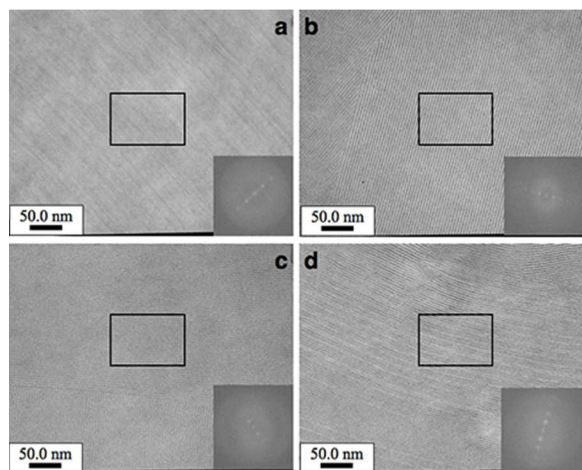
Figure 5. TEM images of thermally annealed samples obtained by decreasing the temperature from the isotropic state to 30ºC at 0.1ºC/min: (a) POSS-C_6-3A; (b) POSS-C_{12}-3A; (c) POSS-C_{18}-2A and (d) POSS-C_{18}-1A. FFT patterns are also shown as the inset in each figure. The magnified TEM images of selected domains are shown in Figure 6.

Hence, we can propose a model for the self-assembled packing of this series of mono-substituted POSS derivatives with long alkyl chains, which is shown schematically in Figure 7. This model is similar to alkylated fullerenes proposed by Nakanishi and coworkers[30, 41-43]. Since the interlayer distances revealed by the WAXS and TEM analyses are significantly less than twice the molecular size, a bilayered self-assembly model is suggested in which POSS molecules pack in a nonstaggered arrangement with interdigitation of the long alkyl chains. Within the POSS-containing layer, the silsesquioxane cages are arranged in a highly organized fashion with a "head-to-head" bilayered structure and a distance around 1.1 nm (refer to the WAXS profiles in the supporting information). Clearly, the POSS molecules arranged in tadpole-like structures as depicted in Figure 7 could form dense molecular packing coincide with the lamellar structure observed from the TEM images.
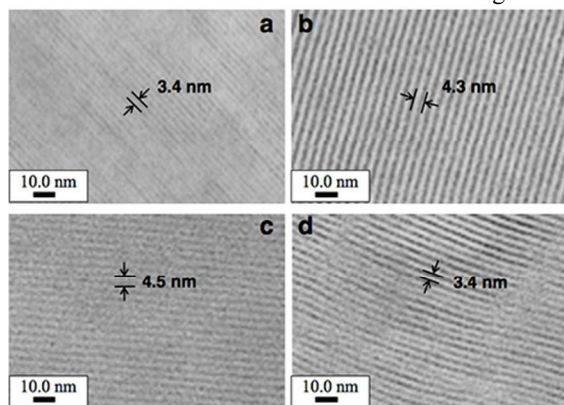

Figure 6. Magnified TEM images of (a) POSS-C_6-3A; (b) POSS-C_{12}-3A; (c) POSS-C_{18}-2A and (d) POSS-C_{18}-1A.

Due to the strong chemical incompatibility between cage silsesquioxane and aliphatic chains, alkylated POSS derivatives

are versatile to achieve a strong segregation and form self-assembled nanostructure. When the sample was obtained by evaporation from the chloroform solvent, alkylated silsesquioxanes possess conformational degree of freedom[37] and thus leads to the lamellar structure lack of long-range ordering.[48] While, after heat treatment, the molecular arrangement underwent an adjustment to a uniform self-assembled nanostructure at large area.[35] Moreover, in this study, the feature sizes of the self-assembled nanostructure could be regulated between 3.4 and 5.3 nm with high regularity, even though future work remains an investigation of the odd-even effect. The result suggests that this class of mono-substituted alkylated POSS derivatives provides a reliable approach to create highly ordered structures at sub-10 nanometer scale.
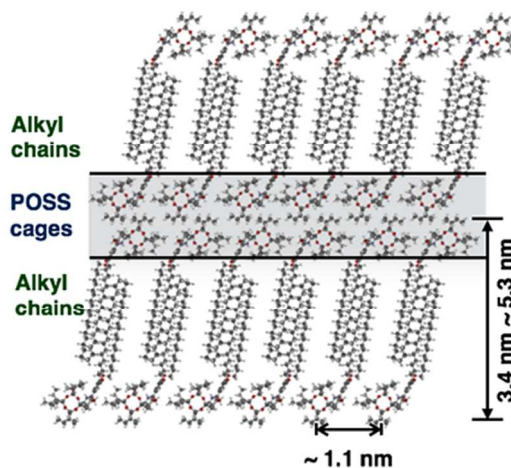

Figure 7. Proposed self-assembled POSS packing model for alkylated POSS derivatives

Conclusions

A series of alkylated cage silsesquioxanes were synthesized and thermal properties as well as self-assembled structures were comprehensive investigated. To three-arm-alkylated POSS, **3** (POSS-C_6-3A) exhibits higher melting temperature and smaller d-spacing than **2** (POSS-C_{12}-3A) and **1** (POSS-C_{18}-3A). While, **5** (POSS-C_{18}-1A) shows the lowest T_m and the smallest periodicity among of C_{18}-substituted cage silsesquioxanes. In brief, attaching alkyl chains of different numbers, and lengths to cage silsesquioxane is proven to be an effective way to tune intermolecular forces and periodicities of molecular packing. In particular, this research provides a guide to the future research of this series of alkylated cage silsesquioxanes from the molecular design perspective. Moreover, these alkylated POSS derivatives can form well-defined lamellar patterns with sub-10 nanometer scale feature sizes. Considering the demands of the microelectronics industry, such long-range straight ordered lamellar structure exhibit potential application in nanofabrication materials.

Acknowledgements

Notes and references

[a]Department of Organic & Polymeric Materials, Tokyo Institute of Technology, Tokyo, Japan

[b]Department of Chemistry, Kanagawa University, Yokohama, Japan

[c]Department of Biochemistry, University of Wisconsin-Madison, Madison, WI, USA

[d]Japan Science and Technology Agency-Precursory Research for Embryonic Science and Technology, JST-PRESTO (Molecular Technology and Creation of New Functions), K's Gobancho Building 7, Gobancho Chiyoda-ku, Tokyo 102-0076, Japan.

†Electronic Supplementary Information (ESI) available: [details of experiments, DSC curves, WAXS profiles, and POM images of alkylated POSS **2**]. See DOI: 10.1039/b000000x/

1   M. Park, C. Harrison, P. M. Chaikin, R. A. Register, D. H. Adamson, *Science,* 1997, **276**, 1401-1404.
2   H.-C. Kim, S.-M. Park, W. D. Hinsberg, *Chem. Rev.,* 2010, **110**, 146-177.
3   Y. Deng, J. Wei, Z. Sun, D. Zhao, *Chem. Soc. Rev.,* 2013, **42**, 4054-4070.
4   M. A. Hillmyer, F. S. Bates, K. Almdal, K. Mortensen, A. J. Ryan, J. P. A. Fairclough, *Science,* 1996, **271**, 976-978.
5   S. B. Darling *Prog. Polym. Sci.,* 2007, **32**, 1152-1204.
6   J. Jarvholm, M. Srinivasarao, L. M. Tolbert, *J. Am. Chem. Soc.,* 2009, **131**, 398-400.
7   C. M. Bates, T. Seshimo, M. J. Maher, W. J. Durand, J. D. Cushen, L. M. Dean, G. Blachut, C. J. Ellison, C. J. Willson, *Science,* 2012, **338**, 775-779.
8   X. Yu, K. Yue, I.-F. Hsieh, Y. Li, X.-H. Dong, Y. Xin, H.-F. Wang, A.-C. Shi, G. R. Newkome, R.-M. Ho, E.-Q. Chen, W.-B. Zhang, S. Z. D. Cheng, *Proc. Natl. Acad. Sci. U. S. A.,* 2013, **110**, 10078-10083.
9   W.-B. Zhang, X. Yu, C.-L. Wang, H.-S. Sun, I.-F. Hsieh, Y. Li, X.-H. Dong, K. Yue, R. V. Horn, S. Z. D. Cheng, *Macromolecules,* 2014, 47, 1221-1239..
10 X. Yu, S. Zhong, X. Li, Y. Tu, S. Yang, R. M. Van Horn, C. Ni, D. J. Pochan, R. P. Quirk, C. Wesdemiotis, W.-B. Zhang, S. Z. D. Cheng *J. Am. Chem. Soc*., 2010, **132**, 16741-16744.
11 Y. Li, K. Guo, H. Su, X. Li, X. Feng, Z. Wang, W. zhang, S. Zhu, C. Wesdemiotis, S. Z. D. Cheng, W.-B. Zhang, *Chem. Sci.,* 2014, **5**, 1046-1053.
12 H. Su, Y. Li, K. Yue, Z. Wang, P. Lu, X. Feng, X.-H. Dong, S. Zhang, S. Z. D. Cheng, W.-B. Zhang *Polym. Chem.,* 2014, **5**, 3697-3706.
13 W.–B. Zhang, Y.-F. Tu, H.-J. Sun, Y. Kan, G. Xiong, S. Z. D. Cheng, *Sci. China Chem.,* 2012, **55**, 749-754.
14 Y. Li, X.-H. Dong, K. Guo, Z. Wang, C. Wesdemiotis, R. P. Quirk, W.-B. Zhang, S. Z. D. Cheng, *ACS Macro Lett.* 2012, **1**, 834-839.
15 X.-H. Dong, R. Van Horn, Z. Chen, B. Ni, X. Yu, A. Wurm, C. Schick, B. Lotz, W.-B. Zhang, S. Z. D. Cheng, *J. Phys. Chem. Lett*., 2013, **4**, 2356-2360.
16 D. B. Cordes, P. D. Lickiss, F. Rataboul, *Chem. Rev.,* 2010, **110**, 2081-2173.
17 S. W. Kuo, F. C. Chang, *Prog. Polym. Sci.,* 2011, **36**, 1649-1696.
18 L. Wang, W. Du, Y. Wu, R. Xu, D. Yu, *J. Appl. Polym. Sci.,* 2012, **126**, 150-155.
19 Y. J. Lee, J. M. Huang, S. W. Kuo, F. C. Chang, *Polymer*, 2005, **46**, 10056-10065.
20 T. Hirai, M. Leolukman, C. C. Liu, E. Han, Y. J. Kim, Y. Ishida, T. Hayakawa, M. A. Kakimoto, *Adv. Mater.,* 2009, **21**, 4334-4338.
21 M. F. Roll, M. Z. Asuncion, J. Kampf, R. M. Laine, *ACS Nano,* 2008, **2**, 320-326.
22 M. Z. Asuncion, M. Ronchi, H. Abuseir, R. M. Laine, *C. R. Chim.,* 2010, **13**, 270-281.
23 X. Ren, B. Sun, C.-C. Tsai, Y. Tu, S. Leng, K. Li, Z. Kang, R. M. Van Horn, X. Li, M. Zhu, C. Wesdemiotis, W.-B. Zhang, S. Z. D. Cheng, *J. Phys. Chem. B*, 2010, **114**, 4802-4810.
24 Y. C. Lin, S. W. Kuo, *Polym. Chem.,* 2012, **3**, 882-891.
25 Y. C. Lin, S. W. Kuo, *J. Polym. Sci. Part A: Polym. Chem.,* 2011, **49**, 2127-2137.
26 Y. C. Lin, S. W. Kuo, *Polym. Chem.,* 2011, **3**, 162-171.
27 J. Miao, L. Zhu, *J. Phys. Chem. B,* 2010, **114**, 1879-1887.
28 C. Zhang, T. J. Bunning, R. M. Laine, *Chem. Mater.,* 2011, **13**, 3653-3662.
29 Q. Pan, X. Chen, X. Fan, Z. Shen, Q. Zhou, *J. Mater. Chem.,* 2008, **18**, 3481-3488.
30 T. Nakanishi, T. Michinobu, K. Yoshida, N. Shirahata, K. Ariga, H. Mohwald, D.G. Kurth, *Adv. Mater.,* 2008, **20**, 443-446.
31 Y. El Aziz, A. R. Bassindale, P. G. Taylor, R. A. Stephenson, M. B. Hursthouse, R. W. Harrington, W. Clegg, *Macromolecules,* 2013, **46**, 988-1001.
32 F. X. Perrin, T. B. V. Nguyen, A. Margaillan, *Eur. Polym. J.,* 2011, **47**, 1370-1382.
33 C. M. Brick, E. R. Chan, S. C. Glotzer, J. C. Marchal, D. C. Martin, R. M. Laine, *Adv. Mater*., 2007, **19**, 82-86.
34 E. L. Heeley, D. J. Hughes, Y. El Aziz, P. G. Taylor, A. R. Bassindale, *Macromolecules,* 2013, **46**, 4944-4954.
35 L. Wang, Y. Ishida, R. Maeda, M. Tokita, S. Horiuchi, T. Hayakawa, *Langmuir*, DOI: 10.1021/la501728z.
36 E. B. Sirota, A. B. Herhold, *Polymer,* 2000, **41**, 8781-8789.
37 E. L. Heeley, D. J. Hughes, Y. El Aziz, I. Williamson, D. G. Taylor, A. R. Bassindale, *Phys. Chem. Chem. Phys.,* 2013, **15**, 5518-5529.
38 E. L. Heeley, D. J. Hughes, Y. El Aziz, D. G. Taylor, A. R. Bassindale, *Eur. Polym. J.,* 2014, **51**, 45-56.
39 X. Wang, C. M. Cho, W. Y. Say, A. Y. X. Tan, C. He, H. S. O. Chan, J. Xu, *J.Mater. Chem.,* 2011, **21**, 5248-5257.
40 T. Ye, X. Chen, X. Fan, Z. Shen, *Soft Matter,* 2013, **9**, 4715-4724.
41 T. Nakanishi, K. Ariga, T. Michinobu, Y. Yoshida, H. Takahashi, T. Teranishi, H. Mohwald, D. G. Kurth, *Small,* 2007, **3**, 2019-2033.
42 H. Li, J. Choi, T. Nakanishi, *Langmuir,* 2013, **29**, 5394-5406.
43 T. Nakanishi, N. Miyashita, T. Michinobu, Y. Wakayama, T. Tsuruoka, K. Ariga, D. G. Kurth, *J. Am. Chem. Soc.,* 2006, **128**, 6328-6329.
44 R. Boese, H.-C. Wesis, D. Blaser, *Angew. Chem. Int. Ed.,* 1999, **38**, 988-992.
45 M. B. Hu, Z.Y. Hou, W. Q. Hao, Y. Xiao, W. Yu, C. Ma, L. J. Ren, P. Zheng, W. Wang. *Langmuir,* 2013, **29**, 5714-5722.
46 H. Li, S. S. Babu, S. T. Turner, D. Neher, M. J. Hollamby, T. Seki, S. Yagai, Y. Deguchi, H. Mohwald, T. Nakanishi, *J. Mater. Chem. C,* 2013, **1**, 1943-1951.
47 M. R. Molla, A. Das, S. Ghosh, *Chem. Commun.,* 2011, **47**, 8934-8936.
48 Y.-F. Lee, K.-H. Chang, C.-Y. Chu, H.-L. Chen, C.-C. Hu, *RSC Advances*, 2011, **1**, 401-407.

Graphical Abstract:
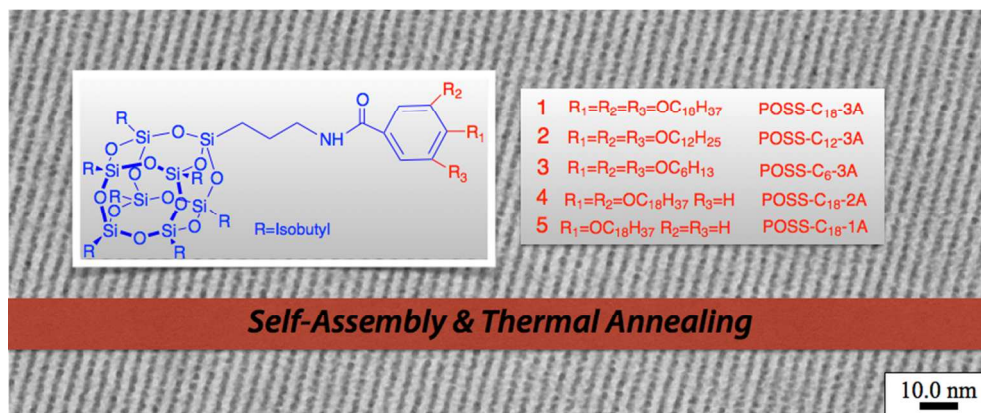
Long-range straight ordered lamellar structures with controllable feature sizes at sub-10 nm scale are created by thoroughly choosing the aliphatic chain length and branch numbers of alkylated cage silsesquioxane.